ECOS 2026: (Iso)butane/CO_2 Zeotropic Mixtures for ORC-Based Carnot Batteries: Efficiency, Robustness, and Pressure Levels

Majid Zarif Sabbaghnia[a], Burak Atakan[b]

[a] University of Duisburg-Essen, Thermodynamics (EMPI), Duisburg, Germany, majid.zarif@uni-due.de , CA

b University of Duisburg-Essen, Thermodynamics (EMPI), Duisburg, Germany, burak.atakan@uni-due.de

Abstract:

Energy storage systems are essential for balancing supply and demand in future electricity systems. In Carnot batteries, electricity is stored as thermal energy and recovered via a heat engine, but in systems with sensible thermal storage the round-trip efficiency (RTE) is often limited by exergy losses in the heat exchangers caused by temperature mismatch. Zeotropic working-fluid mixtures can mitigate these losses through temperature glide during phase change.

This study investigates butane/CO_2 and isobutane/CO_2 mixtures for a standalone Rankine-based Carnot battery consisting of a heat pump for charging, an Organic Rankine Cycle (ORC) for discharging, and sensible hot and cold storages. The charging-cycle performance is adopted from previous work, while the ORC is optimized here with respect to pressure level for different mixture compositions and storage temperatures. In addition, the sensitivity of the system to storage heat losses is analysed.

The results show that increasing the CO_2 mole fraction substantially improves temperature matching in the condensers and thereby increases ORC efficiency and RTE, although at the cost of higher operating pressures and less favourable evaporator matching. The best overall ORC performance is obtained at intermediate-to-high CO_2 fractions, namely for butane/CO_2 (0.20/0.80) and isobutane/CO_2 (0.30/0.70), for which thermal efficiencies of 6.9% and 7.3%, respectively, are achieved at a hot-storage temperature of 383.15 K. Under the same conditions, the corresponding RTE reaches about 24.9% for butane/CO_2 and 26.3% for isobutane/CO_2. Higher hot-storage temperatures further improve ORC efficiency and RTE. Robustness analysis shows that the best-performing mixtures remain favourable under storage losses, but also exhibit a stronger relative sensitivity to deviations from the design storage temperatures.

Overall, hydrocarbon/CO_2 zeotropic mixtures provide a promising compromise between thermal matching, efficiency, and pressure level for standalone ORC-based Carnot batteries with sensible storage.

Keywords:

Carnot Batteries; Round-trip efficiency; Optimization; Zeotropic mixtures; Robustness.

1. Introduction

In future electricity systems, energy storage technologies are essential for balancing temporal mismatches between power generation and demand and for enabling high shares of variable renewable energy. According to the International Energy Agency, electrification and flexibility options such as storage are key elements of decarbonized energy systems [1].

Among large-scale storage concepts, pumped thermal energy storage (PTES), also referred to as Carnot batteries (CBs), has attracted increasing attention. In these systems, electricity is stored as thermal energy during charging and converted back into electricity during discharging. Rankine-based Carnot batteries typically combine a heat pump for charging with an Organic Rankine Cycle (ORC) for discharging. Owing to the use of established thermodynamic components and low-cost thermal storage media, such systems are considered promising for medium- to large-scale stationary energy storage [2–4]

For Carnot batteries using sensible thermal energy storage, the overall performance is often limited by exergy losses in the heat exchangers. Because the storage media undergo non-isothermal temperature changes, significant temperature mismatches may occur during evaporation and condensation, especially in standalone systems with large temperature lifts. Previous studies on Rankine-based Carnot batteries have shown that

heat exchangers account for a major share of the irreversibilities and that the choice of working fluid strongly affects the achievable round-trip efficiency (RTE): Liu et al. [5] investigated R1233zd(E) in a Rankine-based CB with water storage temperatures of 90–130 °C, achieving RTE values of 17–25%, while identifying heat exchangers as the main source of exergy losses (~60%). Similarly, Fan and Xi [6] reported an optimal RTE of 43% using R245fa and R1336mzz in thermally integrated CB configurations, again highlighting heat exchangers as the dominant source of inefficiencies. Eppinger et al. [7] also identified R1233zd(E) as a promising working fluid, reporting RTE values above 60% for small-scale systems.

In this context, natural working fluids are of particular interest. Hydrocarbons offer favorable thermodynamic properties and have shown promising performance in ORC and heat-pump applications, but their use in large-scale systems is limited by flammability and, in some cases, by restricted suitability for large temperature lifts [8], [9]. One promising way to improve temperature matching in systems with sensible storage is the use of zeotropic mixtures. Due to their temperature glide during phase change, such mixtures can reduce irreversibilities in heat exchangers and thereby improve cycle performance. Recent studies have reported beneficial effects of zeotropic mixtures in high-temperature heat pumps, ORCs, and Carnot-battery-related applications. Guo et al. [10] reported an average COP improvement of 5.5% by blending CO_2 with R32, R143a, and R41 for temperature lifts of up to 85 K. Similarly, COP values above 3.5 were achieved for temperature lifts of approximately 110 K using CO_2/butane mixtures [11]. In ORC systems, Huster et al. [12] showed that isobutane/isopentane mixtures can increase net power output by 17% compared to pure fluids. In Carnot batteries, Li et al. [13] reported RTE improvements of 13–20% using R1234yf/isobutane mixtures, along with higher achievable storage temperatures. Qiao et al. [14] identified cyclopentane/R245fa mixtures as optimal for thermally integrated CBs, achieving RTE values above 80% and highlighting heat source temperature as a key influencing parameter.

Transcritical CO_2-based systems represent another important option for large temperature lifts and sensible storage integration. Such systems can achieve favourable temperature matching, but usually require very high operating pressures, often well above 90 bar [15–18]. CO_2-based mixtures may therefore provide an attractive compromise by combining the temperature-glide advantage of mixtures with lower pressure levels than pure transcritical CO_2 cycles. For example, Dai et al.[19] showed that CO_2-based mixtures can improve cycle efficiency while reducing turbine inlet pressure compared with pure CO_2.

From the literature, it follows that hydrocarbons and their mixtures are promising candidates for Rankine-based Carnot batteries in the relevant storage-temperature range, whereas pure or transcritical CO_2 systems are advantageous for large temperature lifts but are associated with high pressure levels. However, only limited work has addressed binary hydrocarbon/CO_2 mixtures in **standalone** Rankine-based Carnot batteries coupled with sensible water-based storage. In addition, the robustness of such systems with respect to storage heat losses has has received little attention.

In previous work, butane/CO_2 and isobutane/CO_2 were identified as particularly promising mixtures for the charging cycle of heat-pump-based thermal storage systems [20]. Building on this, the present study investigates these two mixtures for the discharging process of a standalone Carnot battery consisting of a heat pump, an ORC, and sensible hot and cold storages. Since the thermodynamically favorable mixture composition is not necessarily the same for charging and discharging, the charging-cycle performance is adopted from the previous optimization study, whereas the ORC is optimized here for different mixture compositions and storage temperatures. The objective is to analyze the trade-off between efficiency, pressure level, and robustness against storage heat losses.

2. System and model description

2.1. System configuration

Figure 1 shows the investigated standalone Carnot battery system. It consists of a vapor-compression heat pump for charging, an Organic Rankine Cycle (ORC) for discharging, and two sensible thermal storage units. Water is used as the hot-storage (HS) medium and methanol as the cold-storage (CS) medium; methanol is selected to avoid freezing at sub-ambient temperatures. For each storage, the liquid is pumped from one tank through the corresponding heat exchanger to a second tank. During discharging, the hot-storage fluid is cooled from its nominal storage temperature toward ambient conditions, while the cold-storage fluid is heated toward ambient conditions. During charging, electricity is converted into thermal energy by the heat pump: heat is delivered to the hot storage and extracted from the cold storage. During discharging, the ORC absorbs heat from the hot storage and converts part of it back into electricity, while rejecting heat to the cold storage and, if necessary, to an external sink.

The present work focuses on the discharging process. The charging cycle is not re-optimized here; instead, its performance is adopted from previous work [20], in which several hydrocarbon/CO_2 mixtures were

assessed for heat-pump-based thermal storage. In that study, butane/CO_2 and isobutane/CO_2 were identified as particularly promising candidates. Since the thermodynamically favourable mixture composition differs between charging and discharging, the heat pump and the ORC are treated here as two separate cycles. The coefficient of performance (COP) of the heat pump is therefore taken from Ref [20], whereas the ORC is optimized in the present study.

The charging-cycle assumptions adopted from Ref. [20] are summarized in Table 1. For each selected hot-storage temperature, the corresponding heat-pump COP is used in the round-trip efficiency calculation.

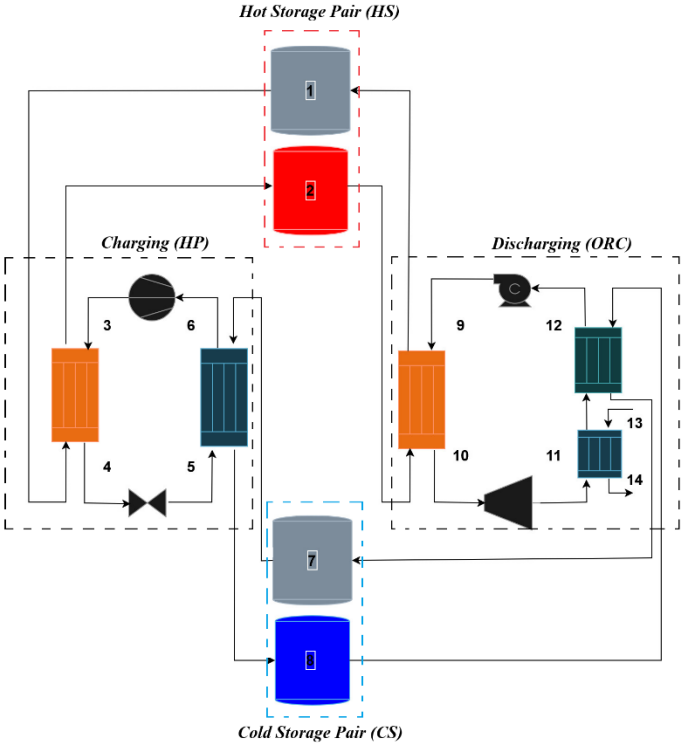

Figure 1. *Flow diagram of the Carnot battery*

Table 1 – Charging cycle assumptions (Heat Pump)

Minimum approach temperature (K)	3.0
Heat Flow Rate ($\dot{Q}_h$) (kW)	1000
Cold storage minimum temperature ($T_{CS,min}$) (K)	273.15
Cold storage maximum temperature ($T_{CS,max}$) (K)	293.15
COP_{HP} at $T_{HS,max}$ = 363.15 K, isobutane/CO_2 (0.85/0.15)	4.11
COP_{HP} at $T_{HS,max}$ = 373.15 K, isobutane/CO_2 (0.80/0.20)	3.83
COP_{HP} at $T_{HS,max}$ = 383.15 K, isobutane/CO_2 (0.90/0.10)	3.62
COP_{HP} at $T_{HS,max}$ = 393.15 K, isobutane/CO_2 (0.90/0.10)	3.48
COP_{HP} at $T_{HS,max}$ = 403.15 K, isobutane/CO_2 (0.90/0.10)	3.37

2.2. Thermodynamic model

The overall performance of the Carnot battery is assessed by the round-trip efficiency (RTE), defined as the ratio of electrical power recovered during discharging to electrical power supplied during charging. In the present formulation, this becomes the product of heat-pump COP and ORC thermal efficiency:

$$RTE = COP_{HP}.\eta_{ORC}.\eta_{St} \quad (1)$$

A steady-state thermodynamic model is applied to the ORC. The cycle is assumed to operate in the subcritical region. Pressure drops in pipes and heat exchangers are neglected, and all heat exchangers are assumed to be isobaric. The pump and expander are described by constant isentropic efficiencies of 90% and 75%, respectively. A minimum approach temperature of 3 K is imposed in all heat exchangers.

During discharging, the hot-storage fluid is pumped to the required pressure and then cooled in the ORC evaporator, where heat is transferred to the working fluid. The working fluid subsequently expands in the expander and generates power. Downstream of the expander, the working fluid is cooled in two condensers arranged in series: first in a water-cooled condenser, then in a condenser coupled to the cold storage, until the fluid reaches the required inlet state of the ORC pump.

The ORC pump power and isentropic efficiency are given by

$$\dot{W}_P - \dot{m}_{WF}.(h_9 - h_{12}) = 0 \quad (2)$$

$$\eta_{Pump} = \frac{\dot{W}_{Pump,s}}{\dot{W}_{Pump}} \quad (3)$$

The evaporator energy balance is given by

$$\dot{m}_{HS}.\left(h_{T_{HS,max}} - h_{T_{HS,min}}\right) - \dot{m}_{WF}.(h_9 - h_{10}) = 0 \quad (4)$$

The expander power and the isentropic efficiency are expressed as

$$\dot{W}_{Exp} - \dot{m}_{WF}.(h_{10} - h_{11}) = 0 \quad (5)$$

$$\eta_{Exp} = \frac{\dot{W}_{Exp}}{\dot{W}_{Exp,s}} \quad (6)$$

The expander is assumed to have a constant isentropic efficiency of 75%. Because the charging and discharging processes are irreversible, the heat rejected during ORC operation is larger than the amount of heat that can be absorbed by the cold storage alone. Therefore, an additional water-cooled condenser is included to reject the excess heat to the environment and to ensure closure of the ORC. The heat that can be transferred to the cold storage is determined from the charging-cycle COP (see Table 1) as

$$\dot{Q}_{CS} = \frac{\dot{Q}_{HS}}{COP_{HP}} \quad (7)$$

The total heat rejected by the ORC is therefore split between the cold-storage condenser and the water-cooled condenser:

$$\dot{Q}_{CT} = \dot{Q}_{CS} + \dot{Q}_{WC} \quad (8)$$

The corresponding energy balance is

$$\dot{m}_{CS}.\left(h_{T_{CS,max}} - h_{T_{CS,min}}\right) + \dot{m}_{WC}.(h_{14} - h_{13}) - \dot{m}_{WF}.(h_{11} - h_{12}) = 0 \quad (9)$$

The ORC thermal efficiency is calculated as

$$\eta_{ORC} = \frac{\dot{W}_{Exp} - \dot{W}_{Pump}}{\dot{Q}_{HS}} \quad (10)$$

and the round-trip efficiency (RTE) of the Carnot battery without storage losses is given by

$$RTE = COP_{HP}.\eta_{ORC} \quad (11)$$

2.3. Optimization and robustness analysis

For each working-fluid composition and each selected hot-storage temperature, the ORC is optimized with respect to the low- and high-pressure levels in order to maximize the thermal efficiency. The optimization variable vector is

$$Y = (P_{min}, P_{max}) \tag{12}$$

whereas the parameter vector is

$$\theta = (x_1, x_2, T_{CS,min}, T_{CS,max}, T_{HS,min}, T_{HS,max}, \Delta T_{pinch}) \tag{13}$$

The optimization problem is formulated as

$$\mathrm{Y}(\theta) = \arg\min[-\eta_{ORC}(Y;\theta)]\,. \tag{14}$$

The lower and upper bounds of the pressure levels are defined from saturation pressures and the minimum pinch-point constraint. The condenser pressure is bounded by

$$P_{Sat,l\,@\,T_{CS,min}+\Delta T_{pinch}} \leq P_{min} \leq 1.35 P_{Sat,l\,@\,T_{CS,min}+\Delta T_{pinch}} \tag{15}$$

$$P_{Sat,l\,@\,T_{HS,min}-\Delta T_{pinch}} \leq P_{max} \leq 1.75 P_{Sat,l\,@\,T_{HS,min}-\Delta T_{pinch}} \tag{16}$$

Here, the subscript Sat,l means the liquid saturated state at the indicated storage temperature and $\Delta T_{\mathrm{pinch}}$ is the prescribed minimum approach temperature.

The optimization is performed using the differential evolution algorithm implemented in pymoo [21], and thermophysical properties are calculated with REFPROP 10.0 [22].

To assess robustness, additional cases are considered in which the storage temperatures deviate from their ideal values due to heat losses to the environment. In the hot storage, heat losses reduce the storage temperature, whereas in the cold storage they increase it. Temperature deviations corresponding to 5%, 10%, and 15% of the difference between storage temperature and ambient temperature are considered. The case with $T_{\mathrm{HS,max}}$=383.15 K is used as the reference condition. The modified storage temperatures are summarized in Table 2. For each loss case, the ORC performance and the resulting RTE are recalculated.

Table 2 – Storage temperatures in different operating conditions

Mode	Hot storage temperature (K)	Cold storage temperature (K)
Ideal	383.15	273.15
5 % loss	378.65	274.15
10 % loss	374.15	275.15
15 % loss	369.65	276.15

3. Results and discussion

3.1. Temperature matching analysis

Zeotropic mixtures undergo non-isothermal phase change and can therefore improve temperature matching with sensible storage media. Based on the initial screening, CO_2 mole fractions between 50% and 90% were found to satisfy the imposed constraints, namely subcritical high-pressure operation, condenser pressures above atmospheric pressure, and compatibility of the saturation lines with the prescribed storage-temperature ranges. To analyse the resulting heat-exchanger behaviour, the optimized cycles are compared using T–$\dot{H}$ diagrams.

For all investigated cases, the hot-storage heat input is fixed at 1000 kW, in accordance with the charging-cycle assumptions adopted from Ref. [19]. In the T–$\dot{H}$ diagrams, the dotted lines represent the external streams, i.e., the hot storage, the cold storage, and the water-cooled condenser, while the solid lines show the corresponding working-fluid temperature profiles in the evaporator and condensers.

Figure 2 and Figure 3 compare the optimized $T–\dot{H}$ diagrams for butane/CO_2 and isobutane/CO_2 mixtures at a hot-storage temperature of 363.15 K. In both cases, the mixture with 50% CO_2 exhibits a pronounced temperature mismatch in the condensation process. Increasing the CO_2 mole fraction to 90% substantially improves the slope matching between the working-fluid condensation line and the sensible cooling/heating lines of the secondary fluids. As a result, the ORC thermal efficiency increases from 4.10% to 4.80% for butane/CO_2 and from 3.87% to 5.02% for isobutane/CO_2.

In addition, higher CO_2 fractions keep the expander outlet further away from the saturation line, so that the expansion ends in a more clearly superheated state.

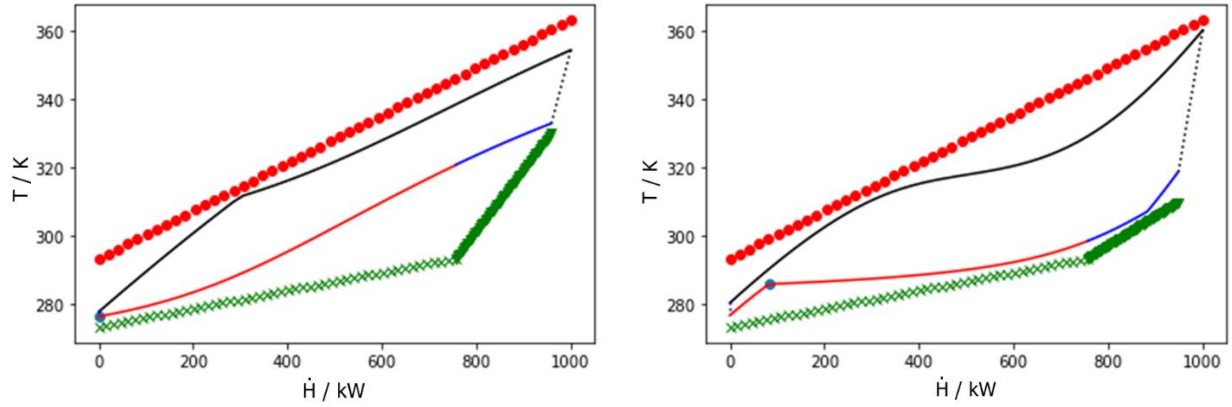

Figure 2. *$T - \dot{H}$ diagrams of butane/CO_2 mixture (0.50/0.50) ($\eta_{ORC} = 4.10\%$) (left) and (0.10/0.90) ($\eta_{ORC} = 4.80\%$) (right) at hot-storage temperatures of 363.15 K.*

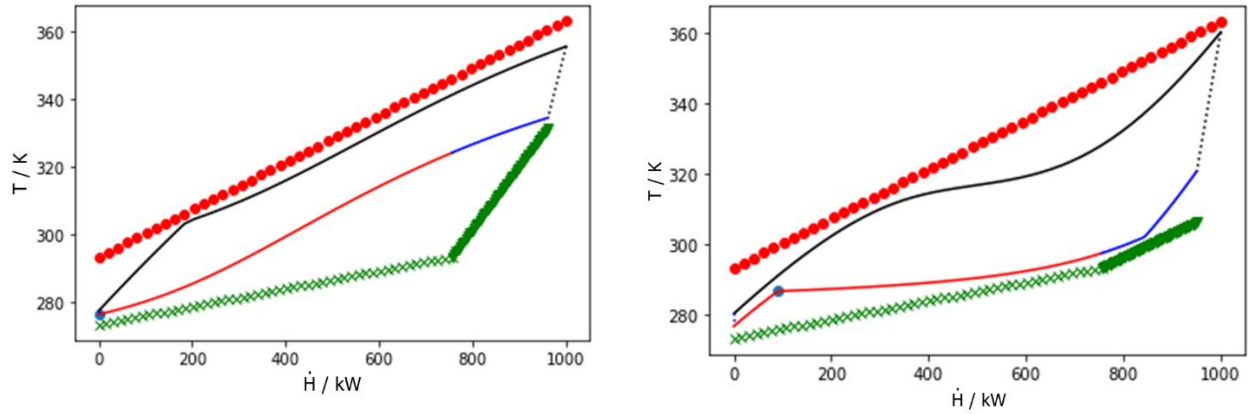

Figure 3 *. $T - \dot{H}$ diagrams of isobutane/CO_2 mixture (0.50/0.50) ($\eta_{ORC} = 3.87\%$) (left) and (0.10/0.90) ($\eta_{ORC} = 5.02\%$) (right) at hot-storage temperatures of 363.15 K.*

To quantify the thermal matching, the mean temperature differences in the three ORC heat exchangers are evaluated. As shown in Figure 4 (right), increasing the CO_2 mole fraction significantly reduces the mean temperature difference in both condensers, whereas the evaporator shows the opposite trend. For the condenser side, the average temperature difference decreases from about 13.5–16 K to approximately 6 K as the CO_2 mole fraction increases from 50% to 80%, before rising slightly again at 90% CO_2.

In contrast, the evaporator mismatch increases by nearly 40%, reaching about 10 K at a CO_2 mole fraction of 70%, and then remains almost constant. Thus, adding CO_2 improves the overall temperature matching mainly through the condensers, while simultaneously worsening the evaporator behaviour. This trade-off explains why the best cycle performance is obtained at intermediate-to-high, but not maximum, CO_2 fractions.

The improved condenser matching is accompanied by higher operating pressures. As shown in Figure 4 (left), both condenser and evaporator pressures increase monotonically with CO_2 content for butane/CO_2 and isobutane/CO_2 mixtures. At a CO_2 mole fraction of 90%, the evaporator pressure approaches 80 bar, while the condenser pressure rises to about 44 bar. On average, the evaporator pressure increases by roughly 10 bar for each additional 10% of CO_2.

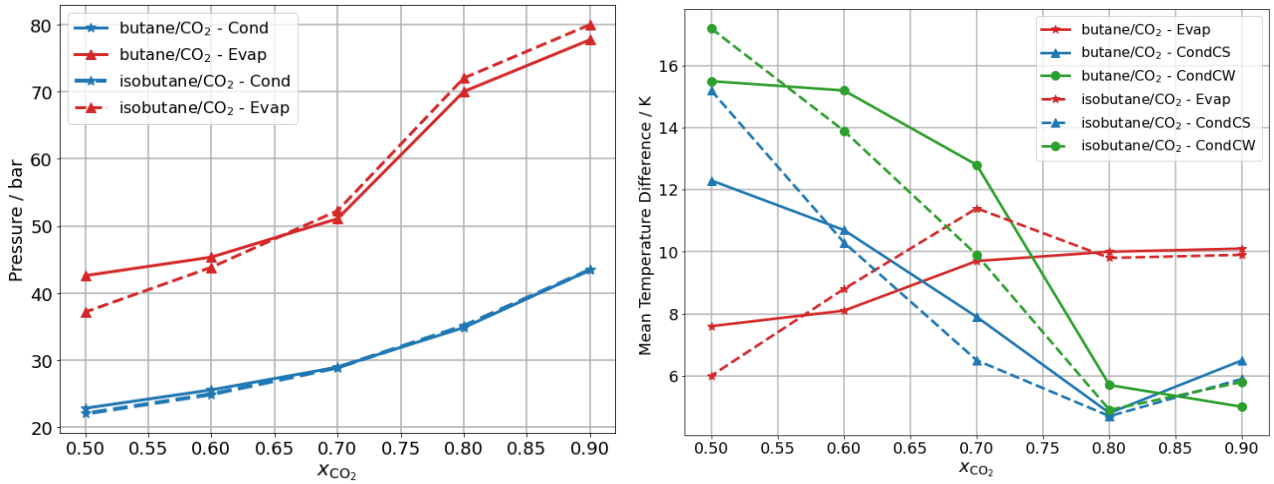

Figure 4. *Pressure levels (left) and mean temperature differences (right) in the heat exchangers as a function of mixture composition at hot-storage temperatures of 363.15 K.*

3.2. Thermodynamic performance analysis

The effects of temperature matching and pressure level are reflected directly in the ORC efficiency and the overall round-trip efficiency (RTE). While increasing the CO_2 content benefits the ORC, the charging-cycle COP adopted from Ref. [20] shows the opposite trend, so that the overall Carnot-battery performance results from a compromise between charging and discharging.

As shown in Figure 5, an optimum composition exists for both mixture families. At a hot-storage temperature of 383.15 K, the ORC thermal efficiency of the butane/CO_2 mixture increases with CO_2 content up to about 80%, where it reaches approximately 7% at an evaporator pressure of about 78 bar, and decreases slightly at 90% CO_2. For isobutane/CO_2, the maximum is obtained at about 70% CO_2, where the thermal efficiency reaches 7.3% at a slightly higher evaporator pressure of around 80 bar.

This behavior is governed by the trade-off identified above. Lower CO_2 fractions provide better temperature matching in the evaporator but poorer matching in the condensers, whereas higher CO_2 fractions improve the condensers at the expense of the evaporator and with a clear pressure penalty. The optimum therefore occurs at CO_2 mole fractions of about 70–80%, where the temperature matching across the full cycle is best balanced.

The RTE trends shown in Figure 6 generally follow the ORC efficiency, but are also shaped by the charging-cycle COP. At 383.15 K, the butane/CO_2 mixture improves from 14.7% at (0.50/0.50) to 24.9% at (0.20/0.80). For the isobutane/CO_2 mixture, the RTE reaches 26.3% at a CO_2 mole fraction of 70%, again with only slightly higher-pressure levels than for the butane-based case.

Increasing the hot-storage temperature improves the ORC thermal efficiency for all investigated mixtures. However, the benefit is most pronounced near the optimum compositions rather than at the extreme CO_2 fractions. At a CO_2 mole fraction of 50%, raising the hot-storage temperature from 363.15 K to 403.15 K increases the thermal efficiency by about 17–40% and the RTE by roughly 13%. At the optimum compositions, the effect is stronger: for butane/CO_2 (0.20/0.80), the RTE rises from 22.5% to 27.5%, while for isobutane/CO_2 (0.30/0.70), it increases from about 20% to 28% over the same temperature range.

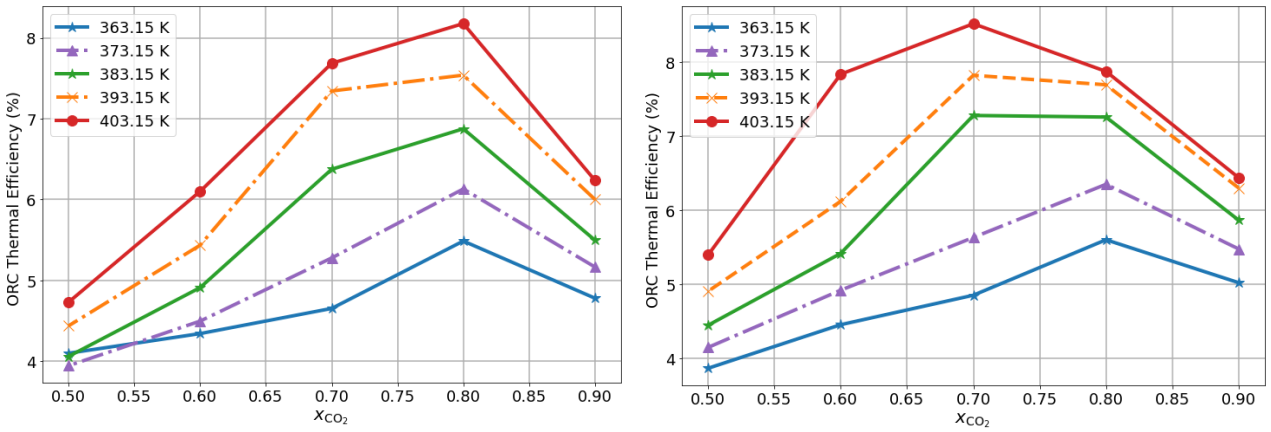

Figure 5. *ORC thermal efficiency butane/CO_2 (left) and isobutane/CO_2 (right) as function of mixture composition and hot-storage temperature.*

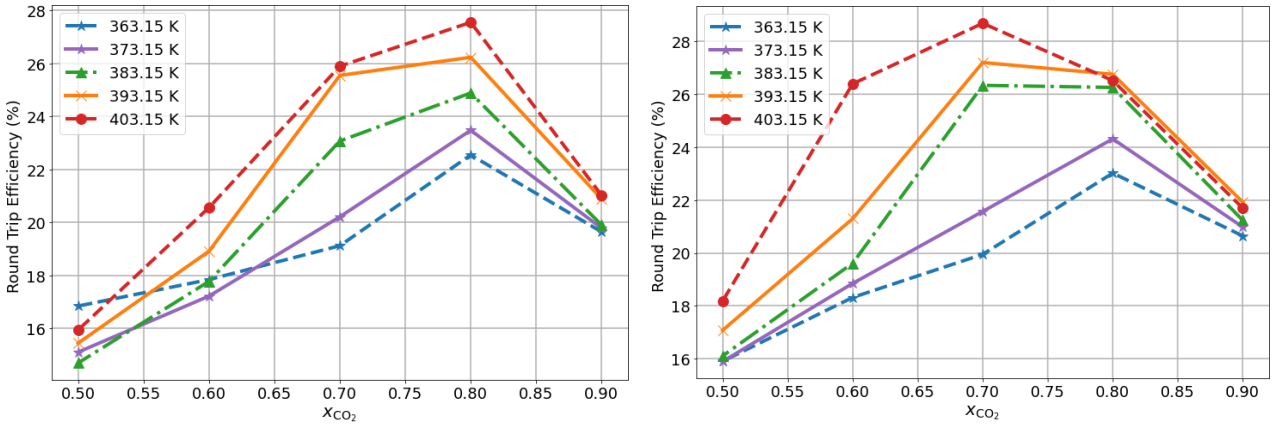

Figure 6. *Round trip efficiency butane/CO_2 (left) and isobutane/CO_2 (right) as function of mixture composition and hot-storage temperature.*

3.3. Robustness Analysis

The robustness of the investigated Carnot battery is assessed by evaluating the sensitivity of the RTE to thermal losses in the storage units. As shown in Figure 7 for the butane/CO_2 mixture, increasing storage losses from 5% to 15% leads to a systematic reduction in RTE across all compositions. For example, at a CO_2 mole fraction of 50%, the RTE decreases from 14.7% under ideal conditions to 11.5% at 15% loss, whereas at 70% CO_2 it drops from about 23% to 15.1%. Thus, compositions near the thermodynamic optimum retain higher absolute efficiencies, but they also show a stronger relative sensitivity to storage losses.

This behavior is illustrated by the $T - \dot{H}$ diagrams in Figure 8 and Figure 9 and 9. For the butane/CO_2 mixture with 80% CO_2, which is close to the thermodynamic optimum, the 15% loss case leads to a visibly stronger distortion of the heat-exchanger temperature profiles than in the 90% CO_2 case. This supports the conclusion that mixtures near the optimum are more sensitive to deviations from the design storage temperatures.

A similar trend is observed for the isobutane/CO_2 mixture, confirming that the effect is not specific to one hydrocarbon. At a CO_2 mole fraction of 50%, the RTE decreases from 16.1% to 12.0% at 15% loss, while at 70% CO_2 it declines from 26.3% to 16.4%. Compared with the butane/CO_2 system, the isobutane/CO_2 mixture therefore shows a slightly higher sensitivity to storage losses, particularly at intermediate CO_2 fractions.

Overall, zeotropic mixtures enhance Carnot-battery performance under ideal conditions, but the robustness analysis shows that the best-performing compositions are also more sensitive to deviations in storage temperature. Nevertheless, the absolute efficiency penalty remains moderate, on the order of 2–6 percentage points, indicating a gradual rather than abrupt deterioration in performance.

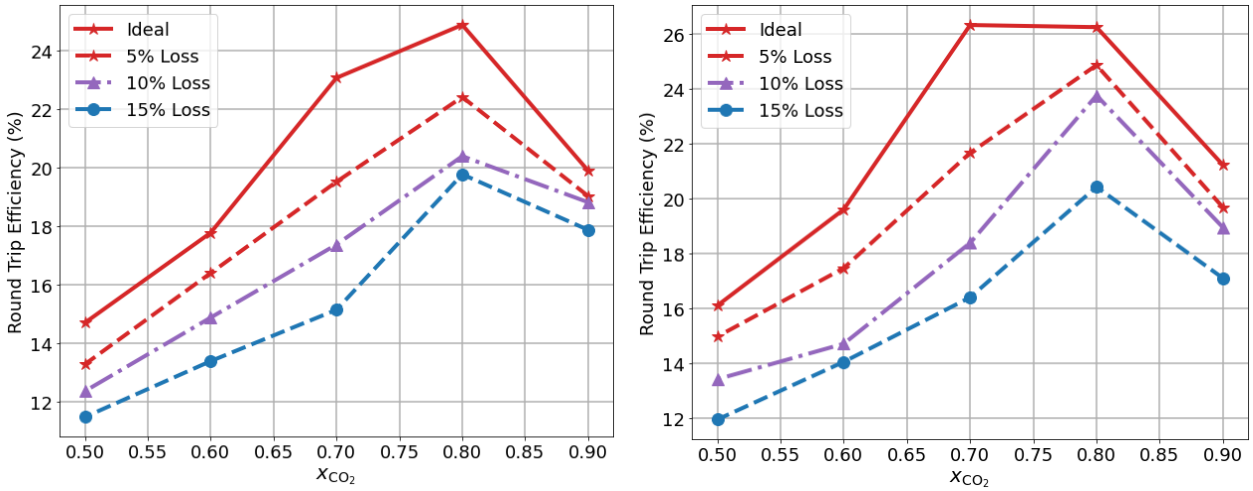

Figure 7. *Round trip efficiency of butane/CO_2 (left) and isobutane/CO_2 (right) as function of mixture composition at storage-loss conditions at a hot-storage temperature of 383.15 K.*

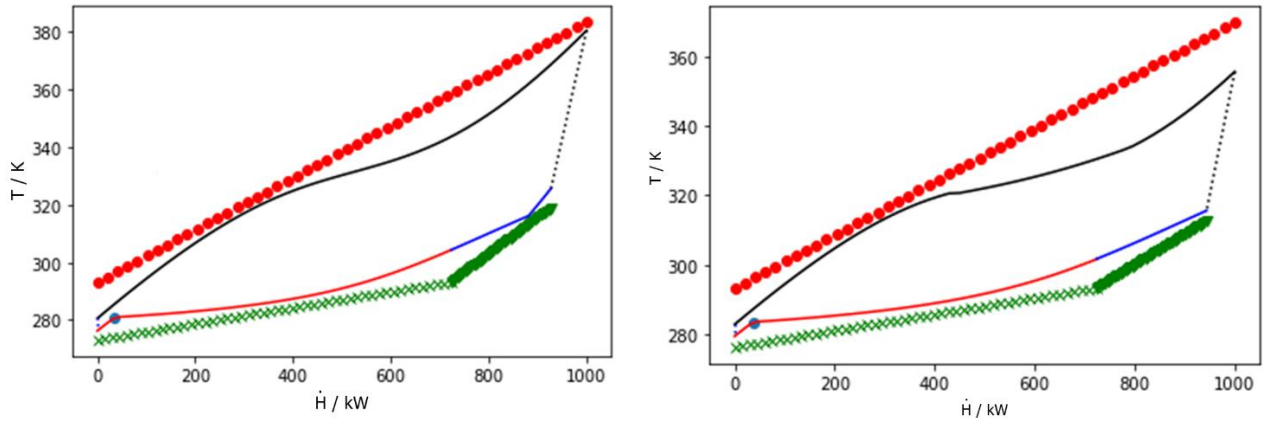

Figure 8. *$T - \dot{H}$ diagram of butane/CO_2 (0.2/0.8) at ideal mode at hot storage temperature of 383.15 K (left) and 15% heat loss mode (right).*

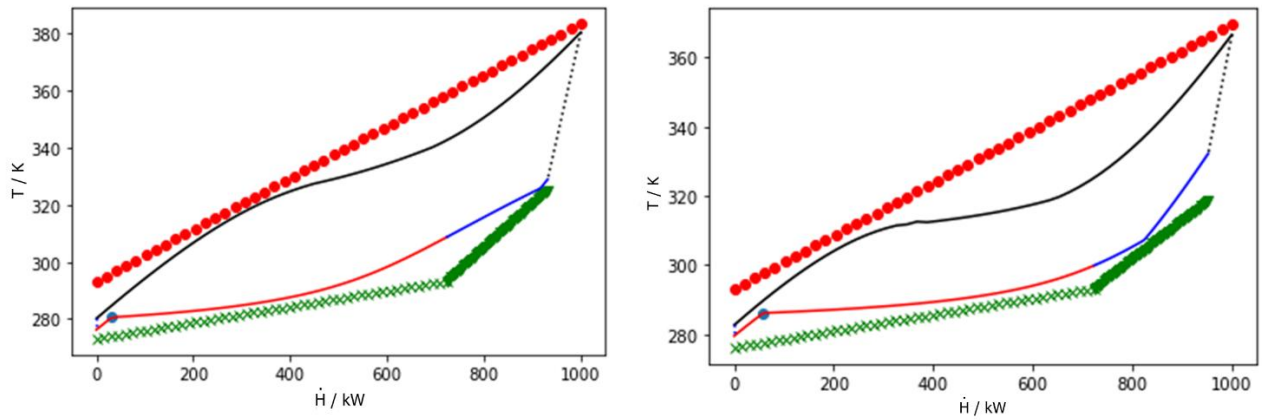

Figure 9. *$T - \dot{H}$ diagram of butane/CO2 (0.1/0.9) at ideal mode at hot storage temperature of 383.15 K (left) and 15% heat loss mode (right).*

4. Conclusions

This study investigated butane/CO_2 and isobutane/CO_2 zeotropic mixtures for the discharging cycle of a standalone Carnot battery consisting of a heat pump, an ORC, and sensible hot and cold storages. The charging-cycle performance was adopted from previous work, while the ORC was optimized with respect to pressure level for different mixture compositions and storage temperatures. The main findings are as follows:

- Increasing the CO_2 content improves temperature matching in the ORC condensers and thereby enhances the thermal efficiency of the discharging cycle. At the same time, the evaporator temperature matching becomes less favourable and the operating pressures increase.
- As a result, the best performance is obtained at intermediate-to-high CO_2 fractions rather than at the maximum CO_2 content. The thermodynamic optimum is found at about 80% CO_2 for butane/CO_2 and about 70% CO_2 for isobutane/CO_2.
- Higher hot-storage temperatures improve both ORC efficiency and round-trip efficiency. The highest RTE values are obtained at the upper end of the investigated storage-temperature range.
- The pressure penalty associated with increasing CO_2 content is substantial: near the optimum region, evaporator pressures approach about 80 bar, while condenser pressures exceed 40 bar.
- Storage heat losses reduce the RTE for all mixtures. Compositions near the thermodynamic optimum remain the best-performing options in absolute terms, but they also show a stronger relative sensitivity to deviations from the design storage temperatures.

Overall, hydrocarbon/CO_2 mixtures offer a promising compromise for standalone Rankine-based Carnot batteries with sensible storage. They improve thermal matching and overall performance compared with lower-CO_2 mixtures, while avoiding the very high pressures typically associated with pure transcritical CO_2 systems.

Acknowledgment

The authors gratefully acknowledge the financial support by the Deutsche Forschungsgemeinschaft (DFG), within the framework of the DFG priority program SPP 2403 Carnot-Batteries: Inverse Design from Markets to Molecules.” and thanks for the scholarship from the German Academic Exchange Service (DAAD).

Nomenclature

COP	Coefficient of performance	(-)	T	Temperature	(K)
h	Specific enthalpy	(kJ/kg)	$\dot{W}$	Power	(kW)
$\dot{H}$	Enthalpy flow rate	(kW)	x	Mole fraction	(-)
$\dot{m}$	Mass flow rate	(kg/s)	Y	Function, Vector	(-)
$\dot{Q}$	Heat transfer rate	(kW)			
RTE	Round Trip Efficiency	(-)			

Greek Symbols

θ	Vector	(-)
η	Thermal efficiency	(-)

Subscripts and superscripts

CS	Cold Storage	min	minimum
Exp	Expander	$pump,s$	Isentropic pump
Exp,s	Isentropic expander	$pump$	pump
ORC	Organic Rankine Cycle	sat,l	Saturation liquid
HP	Heat pump	WC	Water cooled
HS	Hot storage	WF	Working Fluid
max	maximum		

References

[1] International Energy Agency (IEA), “Batteries and Secure Energy Transitions,” International Energy Agency (IEA), Paris, France, 2024. [Online] Available: https://www.iea.org/reports/batteries-and-secure-energy-transitions.

[2] V. Novotny, V. Basta, P. Smola, and J. Spale, “Review of Carnot Battery Technology Commercial Development,” *Energies*, vol. 15, no. 2, p. 647, 2022.

[3] M. Abarr, B. Geels, J. Hertzberg, and L. D. Montoya, “Pumped thermal energy storage and bottoming system part A: Concept and model,” *Energy*, vol. 120, pp. 320–331, 2017.

[4] O. Dumont, G. F. Frate, A. Pillai, S. Lecompte, M. de paepe, and V. Lemort, “Carnot battery technology: A state-of-the-art review,” *Journal of Energy Storage*, vol. 32, p. 101756, 2020.

[5] S. Liu, H. Bai, P. Jiang, Q. Xu, and M. Taghavi, “Economic, energy and exergy assessments of a Carnot battery storage system: Comparison between with and without the use of the regenerators,” *Journal of Energy Storage*, vol. 50, p. 104577, 2022.

[6] R. Fan and H. Xi, “Exergoeconomic optimization and working fluid comparison of low-temperature Carnot battery systems for energy storage,” *Journal of Energy Storage*, vol. 51, p. 104453, 2022.

[7] B. Eppinger, L. Zigan, J. Karl, and S. Will, “Pumped thermal energy storage with heat pump-ORC-systems: Comparison of latent and sensible thermal storages for various fluids,” *Applied Energy*, vol. 280, p. 115940, 2020.

[8] K. Harby, “Hydrocarbons and their mixtures as alternatives to environmental unfriendly halogenated refrigerants: An updated overview,” *Renewable and Sustainable Energy Reviews*, vol. 73, pp. 1247–1264, 2017.

[9] R. S. El-Emam and I. Dincer, “Exergy and exergoeconomic analyses and optimization of geothermal organic Rankine cycle,” *Applied Thermal Engineering*, vol. 59, no. 1-2, pp. 435–444, 2013.

[10] H. Guo, M. Gong, and X. Qin, “Performance analysis of a modified subcritical zeotropic mixture recuperative high-temperature heat pump,” *Applied Energy*, vol. 237, pp. 338–352, 2019.

[11] M. Zarif Sabbaghnia and B. Atakan, Eds., *Butane/CO2 mixture optimization for heat pump based thermal energy storages*. Paris, France: 38th International conference on efficiency, cost, optimization, simulation and environmental impact of energy systems (ECOS), 2025.

[12] W. R. Huster, A. M. Schweidtmann, and A. Mitsos, “Globally optimal working fluid mixture composition for geothermal power cycles,” *Energy*, vol. 212, p. 118731, 2020.

[13] Y. Li, P. Hu, H. Ni, K. Mu, and Y. Ma, “Performance analysis and optimisation of waste heat recovery system based on zeotropic working fluid,” *Applied Thermal Engineering*, vol. 253, p. 123799, 2024.

[14] H. Qiao, X. Lu, L. Yuan, H. Wang, B. Yang, and X. Yu, “Thermodynamic performance analysis and optimization for a Rankine-based Carnot battery utilizing zeotropic mixtures,” *Energy Conversion and Management*, vol. 350, p. 121009, 2026.

[15] M. Morandin, F. Maréchal, M. Mercangöz, and F. Buchter, “Conceptual design of a thermo-electrical energy storage system based on heat integration of thermodynamic cycles – Part B: Alternative system configurations,” *Energy*, vol. 45, no. 1, pp. 386–396, 2012.

[16] F. Ayachi, N. Tauveron, T. Tartière, S. Colasson, and D. Nguyen, “Thermo-Electric Energy Storage involving CO2 transcritical cycles and ground heat storage,” *Applied Thermal Engineering*, vol. 108, pp. 1418–1428, 2016.

[17] J. Bodner, J. Koksharov, F. Dammel, and P. Stephan, “Analysis of low-temperature pumped thermal energy storage systems based on a transcritical CO 2 charging process,” *Energy Science & Engineering*, 2023.

[18] M. Morandin, M. Mercangöz, J. Hemrle, F. Maréchal, and D. Favrat, “Thermoeconomic design optimization of a thermo-electric energy storage system based on transcritical CO2 cycles,” *Energy*, vol. 58, pp. 571–587, 2013.

[19] B. Dai, M. Li, and Y. Ma, “Thermodynamic analysis of carbon dioxide blends with low GWP (global warming potential) working fluids-based transcritical Rankine cycles for low-grade heat energy recovery,” *Energy*, vol. 64, pp. 942–952, 2014.

[20] M. Zarif Sabbaghnia and B. Atakan, “Techno-Economic Analysis of Hydrocarbon-CO 2 Binary Mixtures in Heat Pump-Based Thermal Energy Storages,” *Energy Tech*, vol. 14, no. 4, 2026.

[21] J. Blank and K. Deb, “Pymoo: Multi-Objective Optimization in Python,” *IEEE Access*, vol. 8, pp. 89497–89509, 2020.

[22] *NIST standard reference database 23: reference fluid thermodynamic and transport properties-REFPROP, Version 10.0, National Institute of Standards and …*, 2018.